Sulforaphene suppressed cell proliferation and promoted apoptosis of COV362 cells in endometrioid ovarian cancer

Hui-Yan Yu [1], **Li Yang** [1], **Yuan-Cai Liu** [2], **Ai-Jun Yu** [Corresp. 1]

[1] The Cancer Hospital of the University of Chinese Academy of Sciences (Zhejiang Cancer Hospital), Zhejiang, China, Zhejiang, Zhejiang, China

[2] Zhejiang Chinese Medical University, Zhejiang, China, Zhejiang, Zhejiang, China

Corresponding Author: Ai-Jun Yu
Email address: Yaj1993@126.com

Aim: N6-methyladenosine (m6A) RNA methylation exerts a regulatory effect on endometrioid ovarian cancer (EOC), but the specific m6A regulator genes in EOC remain to be explored. This study investigated that sulforaphene (Sul) is implicated in EOC development by regulating methyltransferase-like 3 (METTL3). **Methods:** The dysregulated m6A RNA methylation genes in EOC were determined by methylated RNA immunoprecipitation (MeRIP-seq) and RNA sequencing. The roles of METTL3 and/or Sul on viability, proliferative ability, cell cycle, and apoptosis of EOC cells were determined by MTT, colony formation, flow cytometry, and TUNEL staining assay, respectively. The expression of METTL3 and apoptosis-related proteins in EOC cells was detected by quantitative real-time polymerase chain reaction (qRT-PCR) and western blot assays. **Results:** Five m6A RNA methylation regulators (METTL3, ELF3, IGF2BP2, FTO, and METTL14) were differentially expressed in EOC, among which METTL3 had the highest expression level. Silencing METTL3 reduced the clonal expansion and viability of EOC cells, and caused the cells to arrest in the G0/G1 phase. This also promoted apoptosis in the EOC cells and activated the FAS/FADD and mitochondrial apoptosis pathways. In contrast, overexpressing METTL3 had the opposite effect. Sul, in a dose-dependent manner, reduced the viability of EOC cells but promoted their apoptosis. Sul also increased the levels of IGF2BP2 and FAS, while decreasing the levels of KRT8 and METTL3. Furthermore, Sul was able to reverse the effects of METTL3 overexpression on EOC cells.**Conclusions:** Sul could suppress cell proliferation and promote apoptosis of EOC cells by inhibiting the METTL3 to activate the FAS/FADD and apoptosis-associated pathways.

1   **Sulforaphene suppressed cell proliferation and promoted apoptosis of**

2   **COV362 cells in endometrioid ovarian cancer**

3   Hui-Yan Yu[1], Li Yang[1], Yuan-Cai Liu[2], Ai-Jun Yu[1*]

4   [1] The Cancer Hospital of the University of Chinese Academy of Sciences (Zhejiang Cancer

5   Hospital), Zhejiang, China

6   [2] Zhejiang Chinese Medical University, Zhejiang, China

7   *Corresponding author: Ai-Jun Yu; The Cancer Hospital of the University of Chinese Academy

8   of Sciences (Zhejiang Cancer Hospital), Zhejiang, China; No.1 East Banshan Road, Gongshu

9   District, Hangzhou, China, 310022; E-mail: Yaj1993@126.com.

10   Running title: Sulforaphene suppresses EOC via METTL3

Abstract

12   **Aim:** N6-methyladenosine (m6A) RNA methylation exerts a regulatory effect on endometrioid

13   ovarian cancer (EOC), but the specific m6A regulator genes in EOC remain to be explored. This

14   study investigated that sulforaphene (Sul) is implicated in EOC development by regulating

15   methyltransferase-like 3 (METTL3).

16   **Methods:** The dysregulated m6A RNA methylation genes in EOC were determined by

17   methylated RNA immunoprecipitation (MeRIP-seq) and RNA sequencing. The roles of

18   METTL3 and/or Sul on viability, proliferative ability, cell cycle, and apoptosis of EOC cells

19   were determined by MTT, colony formation, flow cytometry, and TUNEL staining assay,

20   respectively. The expression of METTL3 and apoptosis-related proteins in EOC cells was

21   detected by quantitative real-time polymerase chain reaction (qRT-PCR) and western blot assays.

22   **Results:** Five m6A RNA methylation regulators (METTL3, ELF3, IGF2BP2, FTO, and

23   METTL14) were differentially expressed in EOC, among which METTL3 had the highest

24   expression level. Silencing METTL3 reduced the clonal expansion and viability of EOC cells,

25   and caused the cells to arrest in the G0/G1 phase. This also promoted apoptosis in the EOC cells

26   and activated the FAS/FADD and mitochondrial apoptosis pathways. In contrast, overexpressing

27 METTL3 had the opposite effect. Sul, in a dose-dependent manner, reduced the viability of EOC

28 cells but promoted their apoptosis. Sul also increased the levels of IGF2BP2 and FAS, while

29 decreasing the levels of KRT8 and METTL3. Furthermore, Sul was able to reverse the effects of

30 METTL3 overexpression on EOC cells.

31 **Conclusions:** Sul could suppress cell proliferation and promote apoptosis of EOC cells by

32 inhibiting the METTL3 to activate the FAS/FADD and apoptosis-associated pathways.

33 **Keywords:** Endometrioid ovarian cancer; Sulforaphene; Methyltransferase-like 3; FAS; FASL

Introduction

35 About one-tenth of all epithelial ovarian cancers are endometrioid ovarian cancers (EOC), a

36 rare kind of ovarian cancer (OC) (Pierson et al., 2020). The development of EOC is related to

37 endometriosis. Approximately 26% of EOC patients were found to have endometriosis when

38 undergoing surgery, while the probability of endometriosis in the uterus of other tumor patients

39 was less than 6% (Wilbur et al., 2017). Patients with recurrent EOC have a dismal prognosis,

40 although the fact that EOC has a better prognosis than other kinds of OC (Pujade-Lauraine et al.,

41 2016). To further enhance the prognosis of patients with EOC, it is vital to discover safe and

42 efficient medications.

43 Inducing apoptosis is an important way to treat malignant tumors, and it has also become

44 one of the important strategies to treat EOC. As a classical apoptotic mechanism, the FAS/FAS

45 ligand (FASL) pathway has emerged as the primary method of cancer treatment (Peng et al.,

46 2022). It is worth noting that the genetic polymorphism of FAS and FASL, as well as the low or

47 nonexistent expression of the FAS gene in EOC, are coupled to the risk and prognosis of patients

48 with EOC (Li et al., 2013; Chaudhry et al., 2010), which means that focusing on FAS/FASL

49 pathway may be a crucial way to treat EOC. Interestingly, N6-methyl adenine (M6A), a

50 reversible mRNA modification method, has been reported to exert a vital effect on many

51 pathways such as mammalian apoptosis and tumorigenesis (Sun et al., 2019). The methylation

52 process of m6A RNA is mainly controlled by m6A methyltransferase, m6A demethylase, and

53 m6A reading protein. Methyltransferase-like 3 (METTL3) is an m6A methyltransferase, which is

54 the catalytic core of the m6A complex (Gao et al., 2021). A study by Bi et al. pointed out that

55 METTL3 was over-expressed in OC, resulting in a decrease in the apoptosis rate of OC (Bi et al.,

56 2021), which may be attributed to the METTL3-mediated increase of m6A methylation of

57 mRNA related to apoptosis (Xu et al., 2021). Therefore, targeting METTL3 may regulate the

58 alterations of the apoptosis signaling pathway downstream of FAS by mediating the methylation

59 of mRNA.

60   The active component in Cruciferae plants known as sulforaphene (Sul) has been shown to

61 have numerous anticancer properties, including the ability to induce tumor cell apoptosis and

62 suppress tumor cell proliferation (Chatterjee et al., 2016; Pawlik et al., 2017). Additionally, Sul

63 has an anti-cancer function in OC, and the underlying mechanism is connected to the control of

64 the cell cycle and apoptosis (Hudecova et al., 2016; Chang et al., 2013). However, uncertainty

65 exists over whether Sul controls the growth of EOC by a comparable mechanism. Notably, Anna

66 et al. pointed out that the anticancer effect of Sul in breast cancer was associated with the

67 regulation of m6A RNA methylation (Lewinska et al., 2017). Nevertheless, the impact of Sul on

68 methylation regulation of m6A RNA has not been proved in EOC. Therefore, the purpose of this

69 investigation is to establish if Sul can perform an anti-tumor effect by controlling the methylation

70 of mRNA, which is mediated by METTL3.

Materials and Methods

Cell culture

73   Human EOC cell line COV362 was ordered from Nanjing Cobioer Biosciences Co. Ltd

74 (Nanjing, China) and was cultured with DMEM complete medium (CBP50008, Cobioer, China)

75 at 37°C incubator with 5% CO_2.

Clinical specimens

77   EOC samples (n=3) and ovarian endometriosis (OE) samples (n=3) were obtained from

78 patients who underwent surgery at Zhejiang Cancer Hospital and were histopathologically

79 assessed by two trained gynecological pathologists before use in this investigation. Forms for

80 informed consent were signed by all patients. The Zhejiang Cancer Hospital Ethics Committee

81 gave its approval for the collection and analysis of human samples (No. IRB-2021-350).

82 **Methylated RNA Immunoprecipitation (Me-RIP)-sequencing and data analysis**

83 The procedure of sequencing was conducted as previously described (Yang et al., 2022).

84 Total RNA from COV362 cells was extracted using Trizol (T11196, Saint-Bio, China), the

85 purity and integrity of which were determined by Qubit 4 (ThermoFisher, USA) and Bioanalyzer

86 2100 (Agilent, USA). RNA was captured by Dynabeads Oligo (dT) (25-61005, Thermo Fisher,

87 USA), and the obtained RNA was broken into small fragments of about 100 nt and

88 immunoprecipitated with m6A-specific antibodies (202003, Synaptic Systems, Germany). The

89 collected RNA fragments containing m6A modifications were used for the construction of a

90 cDNA library using the dUTP method. Finally, double-ended sequencing was conducted using

91 Illumina Novaseq™ 6000 according to standard procedures. The samples' quality was checked

92 by Fastp software, after which HISAT2 mapped the data onto the genome. With visualization

93 provided by the IGV (Thorvaldsdóttir et al., 2013) program and annotation provided by

94 ChIPseeker (Yu et al., 2015), ExomePeak (Meng et al., 2014) was used for Peak calling analysis

95 and gene difference Peak analysis. StringTie (Pertea et al., 2015) was used for quantification,

96 HOMER and MEME2 were utilized for motif analysis, and edgeR (Robinson et al., 2010) was

97 used for difference analysis.

98 **Cell transfection**

99 Specific small interfering RNA (siRNA) targeting METTL3 (si-METTL3,   si-

100 METTL3#1:AGCTACAGATCCTGAGTTAGAGA,si-

101 METTL3#2:GAGTTGATTGAGGTAAAGCGAGG,   si-METTL3#3:

102 ATGTTGATCTGGAGATAGAGAGC) and its negative control (si-NC) were synthesized by

103 Genscript (China). The overexpression vector for METTL3 was constructed by cloning its full-

104 length sequence into the pcDNA3.1 vector (pcDNA3.1-METTL3, VT1001, Youbio, China). To

105 knock down or over-express METTL3 in cells, the synthesized sequences or plasmids were

106 transfected into COV362 cells by different transfection reagents (11668027 and 13778030,

107 ThermoFisher, USA). Transfection reagents and plasmids or siRNA were diluted in advance

108   with serum-free medium and subsequently mixed and incubated with cells for 48 hours.

Cell treatment

110   The experiment was conducted in three stages. First, the effects of overexpression or

111   silencing of METTL3 on EOC cells were determined by the loss and gain of function experiment.

112   Then, the cells were incubated with different concentrations of sulforaphene (Sul, 20, 40, 60 μM,

113   HY-N2450, MedChemExpress, China) to assess the effect of Sul. Finally, the cells

114   overexpressing METTL3 were incubated with Sul (60 μM) to assess whether Sul could block the

115   effect of pcDNA3.1-METTL3.

Quantitative real-time polymerase chain reaction (QRT-PCR)

117   Total RNA from COV362 cells was extracted using Trizol reagent (Thermo Fisher

118   Scientific, USA). A Nanodrop 2000 instrument (Thermo Scientific) was used to measure RNA

119   concentrations. The cDNA was generated from RNA using an RT reagent Kit (CW2569,

120   CWBIO, China). Thereafter, qPCR was performed using qPCR SuperMix (AQ131, TransGen

121   Biotech, China). It was performed using a CFX Connect system (Bio-rad, USA). at 95 °C for

122   600 s, 95 °C for 10 s, 65 °C for 60 s, 97 °C for 1 s, and 37 °C for 30 s, for a total of 40 cycles.

123   The primer sequences for RT-PCR are displayed as follows: METTL3, Forward: 5′-

124   CCCTATGGGACCCTGACAG-3′, Reverse: 5′-CTGGTTGAAGCCTTGGGGAT-3′; ELF3,

125   Forward: 5′-CCACTCCGGTAGCCTCATGG-3′,   Reverse: 5′-

126   AAACCATCGCTGGGGAAGAG-3′;   IGF2BP2,   Forward: 5′-

127   ACTGCAGGCTAAGGGAGAGA-3′, Reverse: 5′-CGCAGCGGGAAATCAATCTG-3′; FTO,

128   Forward: 5′-TGATCTCAATGCCACCCACC-3′,   Reverse: 5′-

129   TGTGCCTTATCAACCTGGGAG-3′;   METTL14,   Forward: 5′-

130   GTAGCACAGACGGGGACTTC-3′, Reverse: 5′-GCCAGCCTGGTCGAATTGTA-3′; Fas,

131   Forward: 5′-CGGAGTTGGGGAAGCTCTTT-3′, Reverse: 5′-TTTGGTGCAAGGGTCACAGT-

132   3′; KRT8, Forward: 5′-GAATGAATGGGGTGAGCTGGA-3′, Reverse: 5′-

133   TCTGGTTGACCGTAACTGCG-3′;   GAPDH   ,   Forward: 5′-

134   CGGAGTCAACGGATTTGGTCGTAT-3′,   Reverse: 5′-

135 AGCCTTCTCCATGGTGGTGAAGAC-3′. GAPDH was regarded as the internal reference. The

136 $2^{-\Delta\Delta CT}$ method was used for calculating the relative transcription level of the target gene.

137 **Western blot assay**

138   COV362 cells were firstly lysed in RIPA Buffer (T10272, Saint-Bio, China) and

139 centrifuged at 12000×g for 10 min to obtain the supernatant, the concentration of which were

140 evaluated by BCA Assay Kit (34001, Saint-Bio, China). Later, a 10% sodium dodecyl sulfate-

141 polyacrylamide gel electrophoresis (SDS-PAGE) gel was employed for the separation of proteins

142 that were electro-transferred onto a membrane (IPVH00010, Saint-Bio, China). After the non-

143 specific sites were blocked by 5% (w/v) nonfat dry milk, the membrane was reacted with

144 primary antibodies against METTL3 (1:1000, ab195352, Abcam), FAS (1:1000, AF5342,

145 Affinity), phospho-FADD (1:1000, DF2996, Affinity), FADD (1:1000, DF7674, Affinity),

146 Caspase-8 (1:1000, AF6442, Affinity), Caspase-3 (1:1000, AF6311, Affinity), Bcl-2 (1:1000,

147 AF6139, Affinity), Bax (1:1000, AF0120, Affinity), and GAPDH (1:5000, AF7021, Affinity)

148 overnight at 4 ℃. GAPDH was regarded as the internal reference. Following the incubation with

149 secondary HRP-linked anti-rabbit IgG antibody (1:3000, #7074, Cell Signaling Technology) for

150 2 hours, the band signals were detected by a Chemiluminescence imaging system (ChemiScope

151 6000, Clinex, China) equipped with ECL reagent kits (T15139, Saint-Bio, China). Finally, the

152 band intensity was measured by Image J software (Bethesda, MD).

153 **MTT assay**

154   MTT kit (20311, Saint-Bio, China) was employed to determine the cell viability. Briefly,

155 cells were planted into 96-well plates and then treated differently according to the experimental

156 requirements. 20 μL MTT was added to the reaction well and incubated for 4 hours. After the

157 purple crystal was dissolved by the Formazan reagent, the absorbance (570 nm) of the reaction

158 well was determined using a microplate plate reader (SpectraMax Mini, Molecular Devices,

159 USA). The half maximal inhibitory concentration (IC50) of Sul was calculated according to the

160 results.

161 **Colony formation assay**

162   The treated cells were first seeded into a 6-well plate with 1000 cells per well and cultured

163   there for 14 days with a medium change every three days. After the culture, the cells were fixed

164   with paraformaldehyde solution (R23025, Saint-Bio, China) and stained with crystal violet

165   (R21877, Saint-Bio, China), after which the number of colonies was counted under a microscope

166   (ECLIPSE E100, Nikon, Japan).

167   **Cell cycle and apoptosis assay**

168   The cell cycle and apoptotic cells were determined by the Cell cycle kit (R21806, Saint-Bio,

169   China) and Annexin V-FITC/ Propidium Iodide (PI) double staining kit (G003, Nanjing

170   Jiancheng Bioengineering Institute, China), respectively. For cell cycle examination, cells were

171   centrifuged at 1000×g for 5 min and then re-suspended in pre-cooled phosphate buffer saline

172   (PBS). After centrifugation in the same way, the cells were resuspended in precooled 70%

173   ethanol and kept for 2 hours. Then, after washing the cells with PBS, the cells were stained with

174   a PI solution for 30 minutes. The results were analyzed by flow cytometry (CytoFLEX LX,

175   Beckman Coulter, USA). For cell apoptosis examination, cells were centrifuged at 1000×g for 5

176   min and then re-suspended in binding buffer, after which the cells were stained with Annexin V-

177   FITC solution (5 μL) and PI solution (5 μL) for 10 min. The results were analyzed by flow

178   cytometry.

179   **Terminal deoxynucleotidyl transferase dUTP nick end labeling (TUNEL) assay**

180   The TUNEL (red) Cell Apoptosis Detection Kit (G1502, Servicebio, China) was employed

181   to detect the apoptotic cells. Cells were inoculated on chamber slides and then treated differently

182   according to the experimental requirements. The cells were fixed for 20 minutes by adding

183   paraformaldehyde solution to each chamber slide, after which cells were immersed in Triton-X-

184   100 solution (T16608, Saint-Bio, China) for incubation for 5 minutes. After washing the sample

185   with PBS twice, the liquid on the chamber slides was absorbed with filter paper. Each sample

186   was dripped with 50 μL of equalization buffer and incubated for 10 minutes. After washing, the

187   cells were incubated with TdT incubation buffer for 1 hour and then DAPI solution (G1012,

188   Servicebio, China) for 8 minutes. Following dyeing, an anti-fade mounting medium (G1401,

189   Servicebio, China) was used to seal the samples, and the samples were analyzed under a

190   fluorescence microscope (Nikon Eclipse C1, Nikon, Japan).

191   **Statistical analysis**

192   All cell experiments were repeated three times and statistical analysis was realized by

193   adopting SPSS 16.0 software. All the quantitative data are represented as the mean ± standard

194   deviation (SD) in our experiment. Differences among multiple groups were determined via one-

195   way Analysis of variance (ANOVA) with the SNK test. An independent sample T-test was used

196   for heterogeneity of variance. Kruskal-Wallis H test was used for the measurement data that does

197   not conform to normal distribution. Data with differences (probabilities of 0.05 or less for *P-*

198   *values*) were regarded as statistically significant.

199   # Results

200   **METTL3 was overexpressed in EOC**

201   We selected EOC (n=3) and OE (n=3) samples for transcriptome-wide detection of m6A

202   modifications and got the top 100 differentially expressed genes, the differential expression heat

203   map of which were shown in Figure 1A. GO and KEGG analysis revealed that these genes were

204   related to cell proliferation, extracellular matrix, and cancer- and cel-cycle-related pathways

205   (Figure 1B-C). A heat map was created to study differential expression profiles of methylation-

206   related genes in EOC and OE (Figure 1D). Among these methylation-related genes, METTL3,

207   ELF3, IGF2BP2, FTO, and METTL14 were verified to be overexpressed in EOC relative to the

208   OE group, especially the METTL3 (Figure 1E, *P*<0.05).

209   **Silencing METTL3 suppressed the malignant phenotypes of EOC cells**

210   We evaluated the efficiency of si-METTL3 and pcDNA3.1-METTL3 by qRT-PCR and

211   western blot. The results unveiled that all three siRNA had inhibitory effects, among which si-

212   METTL3#1 had the most significant inhibitory effect, so the si-METTL3#1 was used in

213   subsequent experiments (Figure 2A-B, *P*<0.05). At the same time, pcDNA3.1-METTL3

214   successfully promoted the mRNA and protein levels of METTL3 (Figure 2A-B, *P*<0.01). Next,

215   our findings uncovered that si-METTL3 or pcDNA3.1-METTL3 did not significantly affect the

216 cell viability after 24 hours of treatment, but after 48 hours and 72 hours of treatment, the former

217 inhibited the cell viability, while the latter fostered the cell viability (Figure 3C, $P<0.05$).

218 Furthermore, si-METTL3 attenuated the clonal expansion of EOC cells and induced the EOC

219 cells to arrest in the GO/G1 phase, while pcDNA3.1-METTL3 did the opposite (Figure 2D-E,

220 $P<0.05$).

221 **Silencing METTL3 fostered the apoptosis of EOC cells by regulating FAS/FASL pathway**

222 TUNEL assay exhibited that the apoptotic cells were increased by si-METTL3 and were

223 diminished by pcDNA3.1-METTL3 (Figure 3A, $P<0.05$). To further analyze the molecular

224 mechanism of METTL3 leading to the above results, we detected the expression of FAS/FASL

225 pathway-related proteins. Si-METTL3 caused the upregulation of FAS, p-FADD/FADD,

226 caspase-8, caspase-3, Cleaved caspase-8, Cleaved caspase-3, and Bax as well as the

227 downregulation of Bcl-2, while pcDNA3.1-METTL3 did the opposite (Figure 3B, $P<0.05$). All

228 these evidences indicated that silencing METTL3 fostered the apoptosis of EOC cells by

229 regulating the FAS/FASL pathway.

230 **Sul dose-dependently inhibited viability promoted apoptosis and regulated the expression**

231 **of IGF2BP2, FAS, KRT8, and METTL3.**

232 To screen for the working concentration of Sul, we treated EOC cells for different times (24,

233 36, and 48 hours) with different concentrations (40, 60, 80, and 100 μM) of Sul and calculated

234 different IC50 values (Figure 4A), respectively. IC50 values for the three different treatment

235 times were all around 60 μM. The results of flow cytometry illustrated that with the increase of

236 Sul concentration from 20 μM to 60 μM, the apoptosis rate gradually elevated (Figure 4B-C,

237 $P<0.01$). Moreover, the mRNA contents of IGF2BP2 and FAS were upregulated, while those of

238 KRT8 and METTL3 were downregulated as the Sul concentration raised (Figure 4D, $P<0.05$).

239 **Effect of pcDNA3.1-METTL3 on malignant phenotypes of EOC cells was reversed by Sul**

240 To explore whether Sul has an anti-cancer effect by inhibiting METTL3, we treated the

241 cells overexpressing METTL3 with Sul. Interestingly, the increases in cell viability (Figure 5A,

242 $P<0.05$) and clonal expansion capacity (Figure 5B, $P<0.05$) as well as the decreases in apoptosis

243 (Figure 5C, *P*<0.05) induced by pcDNA3.1-METTL3 in COV362 cells were reversed after Sul

244 treatment (Figure 5A-C, *P*<0.01). Furthermore, we found that the effect of METTL3

245 overexpression on the expression levels of FAS, FADD, p-FADD, Bcl-2, Bax, and Cleaved

246 Caspase-3 in COV362 cells was reversed under Sul treatment (Figure 5D, *P*<0.01). To sum up,

247 these results showed that Sul might impede the malignant development of EOC by inhibiting

248 METTL3.

Discussion

250   Accumulated evidence suggests that the dysmethylation of m6A is closely related to the

251 development of OC and, in particular, affects the malignancy and prognosis of OC (Zhang et al.,

252 2021). In this study, we determined that the METTL3 gene is the key gene that affects the

253 development of EOC by combining MeRIP-seq and RNA sequencing. There has been evidence

254 that METTL3 is highly expressed in human OC tissue and is related to lymph node metastasis

255 and high pathological grade (Liang et al., 2020). Additionally, METTL3 is considered to be the

256 primary gene responsible for OC metastasis, which can promote the maturation of miR-126-5p

257 through m6A modification and activate the signal pathway related to survival, foster OC

258 metastasis through m6A modification of TRPC3 mRNA, exert a carcinogenic effect on OC by

259 stimulating AXL translation and epithelial-mesenchymal transformation (Hua et al., 2018; Shen

260 et al., 2022; Bi et al., 2021). Although the role of METTL3 in OC has been completely

261 established, it is unknown if METTL3 functions in the same way throughout the various

262 subtypes of OC. In our study, we mainly focused on EOC, an epithelial ovarian cancer, and

263 found that silent METTL3 could inhibit cell viability and proliferative capacity, promote

264 apoptosis, and induce cell cycle arrest in the G0/G1 phase, indicating that METTL3 performed a

265 similar role in EOC as it did in OC. In addition, Ma et al. pointed out that silencing METTL3 in

266 another epidemiologic ovarian cancer can also weaken cell proliferation and migratory ability

267 and promote cell apoptosis (Ma et al., 2020). These pieces of evidence indicate that METTL3

268 may act in a similar carcinogenic manner in various OC cell subtypes, which undoubtedly helps

269 to improve the robustness of the preclinical research of METTL3 against OC.

270   We also found that silencing METTL3 can activate FAS/FADD apoptosis pathway and

271   apoptosis-related pathway. The combination with FAS FASL can induce apoptosis of Fas-

272   carrying cells, and this process requires the recruitment of FADD to produce active-caspase-8,

273   which cleaves caspase-3 to initiate apoptosis (Sun et al., 2022). Activation of Fas/FADD is the

274   key step to start the external apoptosis process, and the loss of related genes in the Fas/FADD

275   apoptosis pathway will lead to a poor prognosis of OC (Duiker et al., 2010). In our investigation,

276   the expression of FAS, p-FADD/FADD, caspase-8, and caspase-3 was promoted by silencing

277   METTL3, which indicated that silencing METTL3 promoted the apoptosis of EOC cells by

278   triggering FAS/FADD apoptosis pathway. At the same time, we unearthed that silencing

279   METTL3 can also control the production of Bax and Bcl-2, which are the essential proteins in

280   mitochondrial apoptosis. According to the accumulating data, increasing the ratio of Bax/Bcl-2

281   can effectively alleviate the metastasis and development of OC (Zhang et al., 2019; Liu et al.,

282   2017). Previous research has reported that silencing METTL3 can increase the ratio of Bax/Bcl-2,

283   trigger mitochondrial apoptosis, and prevent the development of lung cancer cells (Wei et al.,

284   2019). These effects appear to be related to the inhibition of m6A modification of Bcl-2 by

285   METTL3 (Zhang et al., 2021). Similarly, our findings also suggested that silencing METTL3

286   may promote the apoptosis of EOC cells by triggering the apoptosis pathway by altering the

287   Bax/Bcl-2 signaling pathway.

288   Although Sul has been mentioned in previous articles as an epigenetic regulator with the

289   ability to regulate DNA methyltransferase, histone deacetylase, non-coding RNA, etc (Su et al.,

290   2018), this study marks the first time that Sul has been proven to be capable of targeting m6A

291   methyltransferase METTL3. In addition, although the role of Sul in OC has been extensively

292   covered, its role in EOC has only recently come to light. Consistent with the anticancer effect of

293   Sul in OC (Kan et al., 2018), we found that Sul fostered EOC cell apoptosis and diminished EOC

294   cell proliferative capacity in a concentration-dependent manner. Sul reversed the carcinogenesis

295   of pcDNA3.1-METTL3, which indicated that Sul partly prevented the development of EOC by

296   reducing the expression of METTL3. Furthermore, Sul upregulated the levels of insulin growth

297 factor 2 mRNA binding protein 2 (IGF2BP2) and FAS as well as downregulated the levels of

298 KRT8 and METTL3. IGF2BP2, localized on chromosome 3q27, a m6A-modified reading

299 protein, plays an important role in embryonic development that is lowly expressed in normal

300 adult tissues and can act as a post-transcriptional regulator of mRNA localization, stabilization,

301 and translation by stabilizing mRNAs to extend their half-life, while KRT8 is a marker of

302 epithelium, both of which are reported to be related to the development of OC (Prayudi et al.,

303 2020; Park et al., 2022). The link between METTL3 and KRT8 is yet unknown, however, it

304 appears that IGF2BP2 is necessary for METTL3's regulatory action on m6A modification (Wang

305 et al., 2022). IGF2BP2 is up-regulated in a variety of tumors, and its biological activity

306 contributes to cancer formation by interacting with various non-coding RNAs including

307 microRNAs (miRNAs), long non-coding RNAs (lncRNAs), and circular RNAs (circRNAs)

308 (Wang et al., 2021). It was surprising that the expression of IGF2BP2 increased in COV362 cells

309 treated with Sul. As a result, there may be a part of the intracellular compensatory response in

310 EOC. More importantly, our study also has some limitations. Future studies are necessary to

311 address whether a specific pathway or mechanism by which Sul affects IGF2BP2 directly. And,

312 the more details of clinical trials and basic scientific research need further study in the future.

313   In conclusion, our study shows that the knockdown of METTL3 has significantly inhibited

314 cell proliferation and promoted cell apoptosis *in vitro*, while an opposite effect was observed in

315 COV362 cells with METTL3 overexpression. Additionally, we report that the Sul contributed to

316 an increase in cell apoptosis of COV362 cells, and disrupted the effect of METTL3

317 overexpression on cell proliferation and apoptosis in EOC. These results showed that Sul-

318 induced METTL3-dependent apoptosis, which might be related to the FAS/FADD and Bax/Bcl-

319 2 associated pathway, might provide its clinical potential applications for preventing and treating

320 EOC.

321 Funding Statement

322 This research was funded by the Public Welfare Technology Project of Zhejiang Province

323 (LGF19H160011) and the Zhejiang Provincial Health and Medicine Science and Technology

324 Project (2019ZD001).

Data Availability

326 The following information was supplied regarding data availability: The raw measurements are

327 available in the Supplemental Files.

Competing Interests

329 The authors declare there are no competing interests.

Author contributions

331 HYY and AJY: conceptualization. AJY: funding acquisition. HYY, LY, and YCL: investigation.

332 HYY: writing-original draft. HYY and AJY: writing-review and editing. All authors contributed

333 to the article and approved the submitted version.

References

335 1. Bi et al. (2021) Bi X, Lv X, Liu D, Guo H, Yao G, Wang L, Liang X, Yang Y. METTL3

336   promotes the initiation and metastasis of ovarian cancer by inhibiting CCNG2 expression via

337   promoting the maturation of pri-microRNA-1246. Cell Death Discov. 2021;7(1):237.

338   doi:10.1038/s41420-021-00600-2.

339 2. Bi et al. (2021) Bi X, Lv X, Liu D, Guo H, Yao G, Wang L, Liang X, Yang Y. METTL3-

340   mediated maturation of miR-126-5p promotes ovarian cancer progression via PTEN-

341   mediated PI3K/Akt/mTOR pathway. Cancer Gene Ther. 2021;28(3-4):335-349.

342   doi:10.1038/s41417-020-00222-3.

343 3. Chaudhry et al. (2010) Chaudhry P, Srinivasan R, Patel FD. Expression of the major fas

344   family and Bcl-2 family of proteins in epithelial ovarian cancer (EOC) and their correlation

345   to chemotherapeutic response and outcome. Oncol Res. 2010;18(11-12):549-559.

346   doi:10.3727/096504010x12767359113884.

347 4. Chatterjee et al. (2016) Chatterjee S, Rhee YH, Ahn JC. Sulforaphene-Carboplatin

348   Combination Synergistically Enhances Apoptosis by Disruption of Mitochondrial

349   Membrane Potential and Cell Cycle Arrest in Human Non-Small Cell Lung Carcinoma. J

350   Med Food. 2016;19(9):860-869. doi:10.1089/jmf.2016.3675.

351   5.   Chang et al. (2013) Chang CC, Hung CM, Yang YR, Lee MJ, Hsu YC. Sulforaphane

352   induced cell cycle arrest in the G2/M phase via the blockade of cyclin B1/CDC2 in human

353   ovarian cancer cells. J Ovarian Res. 2013;6(1):41. doi:10.1186/1757-2215-6-41.

354   6.   Duiker et al. (2010) Duiker EW, van der Zee AG, de Graeff P, Boersma-van Ek W, Hollema

355   H, de Bock GH, de Jong S, de Vries EG. The extrinsic apoptosis pathway and its prognostic

356   impact   in   ovarian   cancer.   Gynecol   Oncol.   2010;116(3):549-555.

357   doi:10.1016/j.ygyno.2009.09.014.

358   7.   Gao et al. (2021) Gao R, Ye M, Liu B, Wei M, Ma D, Dong K. m6A Modification: A

359   Double-Edged   Sword   in   Tumor   Development.   Front   Oncol.   2021;11:679367.

360   doi:10.3389/fonc.2021.679367.

361   8.   Hudecova et al. (2016) Hudecova S, Markova J, Simko V, Csaderova L, Stracina T, Sirova

362   M, Fojtu M, Svastova E, Gronesova P, Pastorek M, Novakova M, Cholujova D, Kopacek J,

363   Pastorekova S, Sedlak J, Krizanova O. Sulforaphane-induced apoptosis involves the type 1

364   IP3 receptor. Oncotarget. 2016;7(38):61403-61418. doi:10.18632/oncotarget.8968.

365   9.   Hua et al. (2018) Hua W, Zhao Y, Jin X, Yu D, He J, Xie D, Duan P. METTL3 promotes

366   ovarian carcinoma growth and invasion through the regulation of AXL translation and

367   epithelial   to   mesenchymal   transition.   Gynecol   Oncol.   2018;151(2):356-365.

368   doi:10.1016/j.ygyno.2018.09.015.

369   10. Kan et al. (2018) Kan SF, Wang J, Sun GX. Sulforaphane regulates apoptosis- and

370   proliferation-related signaling pathways and synergizes with cisplatin to suppress human

371   ovarian cancer. Int J Mol Med. 2018;42(5):2447-2458. doi:10.3892/ijmm.2018.3860.

372   11. Li et al. (2013) Li Y, Hao YL, Kang S, Zhou RM, Wang N, Qi BL. Genetic polymorphisms

373   in the Fas and FasL genes are associated with epithelial ovarian cancer risk and clinical

374   outcomes. Gynecol Oncol. 2013;128(3):584-589. doi:10.1016/j.ygyno.2012.12.00.

375   12. Lewinska et al. (2017) Lewinska A, Adamczyk-Grochala J, Deregowska A, Wnuk M.

376   Sulforaphane-Induced Cell Cycle Arrest and Senescence are accompanied by DNA

377   Hypomethylation and Changes in microRNA Profile in Breast Cancer Cells. Theranostics.

378   2017;7(14):3461-3477. doi:10.7150/thno.20657.

379   13. Liang et al. (2020) Liang S, Guan H, Lin X, Li N, Geng F, Li J. METTL3 serves an

380   oncogenic role in human ovarian cancer cells partially via the AKT signaling pathway.

381   Oncol Lett. 2020;19(4):3197-3204. doi:10.3892/ol.2020.11425.

382   14. Liu et al. (2017) Liu X, Dong J, Cai W, Pan Y, Li R, Li B. The Effect of Thymoquinone on

383   Apoptosis of SK-OV-3 Ovarian Cancer Cell by Regulation of Bcl-2 and Bax. Int J Gynecol

384   Cancer. 2017;27(8):1596-1601. doi:10.1097/IGC.0000000000001064.

385   15. Meng et al. (2014) Meng J, Lu Z, Liu H, Zhang L, Zhang S, Chen Y, Rao MK, Huang Y. A

386   protocol for RNA methylation differential analysis with MeRIP-Seq data and exomePeak

387   R/Bioconductor package. Methods. 2014;69(3):274-281. doi:10.1016/j.ymeth.2014.06.008.

388   16. Ma et al. (2020) Ma Z, Li Q, Liu P, Dong W, Zuo Y. METTL3 regulates m6A in

389   endometrioid epithelial ovarian cancer independently of METTl14 and WTAP. Cell Biol Int.

390   2020;44(12):2524-2531. doi:10.1002/cbin.11459.

391   17. Pierson et al. (2020) Pierson WE, Peters PN, Chang MT, Chen LM, Quigley DA, Ashworth

392   A, Chapman JS. An integrated molecular profile of endometrioid ovarian cancer. Gynecol

393   Oncol. 2020;157(1):55-61. doi:10.1016/j.ygyno.2020.02.011.

394   18. Pujade-Lauraine et al. (2016) Pujade-Lauraine E, Combe P. Recurrent ovarian cancer. Ann

395   Oncol. 2016;27 Suppl 1:i63-i65. doi:10.1093/annonc/mdw079.

396   19. Peng et al. (2022) Peng F, Liao M, Qin R, Zhu S, Peng C, Fu L, Chen Y, Han B. Regulated

397   cell death (RCD) in cancer: key pathways and targeted therapies. Signal Transduct Target

398   Ther. 2022;7(1):286. doi:10.1038/s41392-022-01110-y.

399   20. Pawlik et al. (2017) Pawlik A, Wała M, Hać A, Felczykowska A, Herman-Antosiewicz A.

400   Sulforaphene, an isothiocyanate present in radish plants, inhibits proliferation of human

401   breast cancer cells. Phytomedicine. 2017;29:1-10. doi:10.1016/j.phymed.2017.03.007.

402   21. Pertea et al. (2015) Pertea M, Pertea GM, Antonescu CM, Chang TC, Mendell JT, Salzberg

403   SL. StringTie enables improved reconstruction of a transcriptome from RNA-seq reads. Nat

404   Biotechnol. 2015;33(3):290-295. doi:10.1038/nbt.3122.

405 22. Prayudi et al. (2020) Prayudi PKA, Budiana ING, Mahayasa PD, Surya IGNHW,

406   Wiradnyana AAGP, Suwiyoga K. Diagnostic accuracy of serum insulin-like growth factor-

407   binding protein 2 for ovarian cancer. Int J Gynecol Cancer. 2020;30(11):1762-1767.

408   doi:10.1136/ijgc-2020-001479.

409 23. Park et al. (2022) Park ES, Xiang D, Xie Y, Bronson RT, Li Z. Oncogenic Events Dictate

410   the Types and Locations of Gynecological Malignancies Originating from Krt8+

411   Mesothelial and Müllerian-Derived Epithelial Cells. Cancers (Basel). 2022;14(3):841.

412   doi:10.3390/cancers14030841.

413 24. Robinson et al. (2010) Robinson MD, McCarthy DJ, Smyth GK. edgeR: a Bioconductor

414   package for differential expression analysis of digital gene expression data. Bioinformatics.

415   2010;26(1):139-140. doi:10.1093/bioinformatics/btp616

416 25. Sun et al. (2019) Sun T, Wu R, Ming L. The role of m6A RNA methylation in cancer.

417   Biomed Pharmacother. 2019;112:108613. doi:10.1016/j.biopha.2019.108613.

418 26. Shen et al. (2022) Shen Z, Gu L, Liu Y, Wang L, Zhu J, Tang S, Wei X, Wang J, Zhang S,

419   Wang X, Cheng X, Xie X, Lu W. PLAA suppresses ovarian cancer metastasis via METTL3-

420   mediated m6A modification of TRPC3 mRNA. Oncogene. 2022;41(35):4145-4158.

421   doi:10.1038/s41388-022-02411-w.

422 27. Sun et al. (2022) Sun H, Yang Y, Gu M, Li Y, Jiao Z, Lu C, Li B, Jiang Y, Jiang L, Chu F,

423   Yang W, Sun D, Gao Y. The role of Fas-FasL-FADD signaling pathway in arsenic-mediated

424   neuronal apoptosis in vivo and in vitro. Toxicol Lett. 2022;356:143-150.

425   doi:10.1016/j.toxlet.2021.11.012.

426 28. Su et al (2018) Su X, Jiang X, Meng L, Dong X, Shen Y, Xin Y. Anticancer Activity of

427   Sulforaphane: The Epigenetic Mechanisms and the Nrf2 Signaling Pathway. Oxid Med Cell

428   Longev. 2018;2018:5438179. doi:10.1155/2018/5438179.

429 29. Thorvaldsdóttir et al. (2013) Thorvaldsdóttir H, Robinson JT, Mesirov JP. Integrative

430   Genomics Viewer (IGV): high-performance genomics data visualization and exploration.

431   Brief Bioinform. 2013;14(2):178-192. doi:10.1093/bib/bbs017.

432   30. Wilbur et al. (2017) Wilbur MA, Shih IM, Segars JH, Fader AN. Cancer Implications for

433   Patients with Endometriosis. Semin Reprod Med. 2017;35(1):110-116. doi:10.1055/s-0036-

434   1597120.

435   31. Wei et al. (2019) Wei W, Huo B, Shi X. miR-600 inhibits lung cancer via downregulating

436   the   expression   of   METTL3.   Cancer   Manag   Res.   2019;11:1177-1187.

437   doi:10.2147/CMAR.S181058.

438   32. Wang et al. (2022) Wang JN, Wang F, Ke J, Li Z, Xu CH, Yang Q, Chen X, He XY, He Y,

439   Suo XG, Li C, Yu JT, Jiang L, Ni WJ, Jin J, Liu MM, Shao W, Yang C, Gong Q, Chen HY,

440   Li J, Wu YG, Meng XM. Inhibition of METTL3 attenuates renal injury and inflammation by

441   alleviating TAB3 m6A modifications via IGF2BP2-dependent mechanisms. Sci Transl Med.

442   2022;14(640):eabk2709. doi:10.1126/scitranslmed.abk2709.

443   33. Wang et al. (2021) Wang J, Chen L, Qiang P. The role of IGF2BP2, an m6A reader gene, in

444   human metabolic diseases and cancers. Cancer Cell Int. 2021;21(1):99. doi:10.1186/s12935-

445   021-01799-x

446   34. Xu et al. (2021) Xu L, Zhang C, Yin H, Gong S, Wu N, Ren Z, Zhang Y. RNA

447   modifications act as regulators of cell death. RNA Biol. 2021;18(12):2183-2193.

448   doi:10.1080/15476286.2021.1925460.

449   35. Yang et al. (2022) Yang L, Chen X, Qian X, Zhang J, Wu M, Yu A. Comprehensive

450   Analysis of the Transcriptome-Wide m6A Methylome in Endometrioid Ovarian Cancer.

451   Front Oncol. 2022;12:844613. doi:10.3389/fonc.2022.844613.

452   36. Yu et al. (2015) Yu G, Wang LG, He QY. ChIPseeker: an R/Bioconductor package for ChIP

453   peak annotation, comparison and visualization. Bioinformatics. 2015;31(14):2382-2383.

454   doi:10.1093/bioinformatics/btv145.

455   37. Zhang et al. (2021) Zhang C, Liu J, Guo H, Hong D, Ji J, Zhang Q, Guan Q, Ren Q. m6A

456   RNA methylation regulators were associated with the malignancy and prognosis of ovarian

457   cancer. Bioengineered. 2021;12(1):3159-3176. doi:10.1080/21655979.2021.1946305.

458

38. Zhang et al. (2019) Zhang H, Dong R, Zhang P, Wang Y. Songorine suppresses cell growth and metastasis in epithelial ovarian cancer via the Bcl-2/Bax and GSK3β/β-catenin signaling pathways. Oncol Rep. 2019;41(5):3069-3079. doi:10.3892/or.2019.7070.

39. Zhang et al. (2021) Zhang Y, Liu S, Zhao T, Dang C. METTL3-mediated m6A modification of Bcl-2 mRNA promotes non-small cell lung cancer progression. Oncol Rep. 2021;46(2):163. doi:10.3892/or.2021.8114.

Figure legends

Figure 1 Identification of methylation-associated genes in endometrioid ovarian cancer. (A) Representative heatmap of differentially expressed genes between the endometrioid ovarian cancer (EOC) and ovarian endometriosis (OE). (B) Gene Ontology (GO) analysis of differentially expressed genes. (C) Kyoto Encyclopedia of Genes and Genomes (KEGG) analysis of differentially expressed genes. (D) Representative heatmap of methylation-associated genes. (E) Relative expression of methylation-associated genes METTL3, ELF3, IGF2BP2, FTO, and METTL14 in EOC and OE tissues. *P<0.05, **P<0.01 vs. OE group.

Figure 2 Effect of METTL3 on COV362 cell proliferation. (A, B) Relative expression of METTL3 in COV362 cells transfected with siRNA against METTL3 or pcDNA3.1 overexpressed METTL3 was assessed by qPCR and Western blot analysis, respectively. (C) The viability of cells was evaluated by a CCK-8 assay. (D) Colony formation assays were performed in COV362 cells treated with si-NC, si-METTL3, pcDNA3.1, or pcDNA3.1-METTL3. (E) Representative images of the cell cycle in COV362 cells after silencing METTL3 or elevating METTL3 were analyzed by flow cytometry. ▲P<0.05, ▲▲P<0.01 vs. si-NC group; *P<0.05, **P<0.01 vs. PcDNA3.1 group.

Figure 3 Effect of METTL3 on COV362 cell apoptosis. (A) Representative images of cell apoptosis in COV362 cells after silencing METTL3 or elevating METTL3 were analyzed by Tunel staining. scale bar=50 μm. (B) FAS, FADD, p-FADD, Caspase-8, Caspase-3, Cleaved Caspase-8, Cleaved Caspase-3, Bcl-2, and Bax protein expressions were determined in COV362

485   cells with METTL3 knock-down or overexpression through western blotting. ▲*P<0.05*,

486   ▲▲*P<0.01 vs.* si-NC group; *P<0.05, **P<0.01 vs.* PcDNA3.1 group.

487   **Figure 4 Sulforaphene promoted cell apoptosis of COV362 cells.** (A) CCK-8 analysis

488   suggested that the cell viability of COV362 cells was inhibited by a dose-dependent manner of

489   sulforaphene (Sul) treatment. (B) Representative pictures of apoptosis of Sul-treated COV362

490   cells that were measured by FACS analysis. (C) The relative apoptosis rate of COV362 cells

491   treated with the different concentrations of Sul. (D) Effect of different concentrations of Sul on

492   IGF2BP2, FAS, KRT8, and METTL3 mRNA levels, as assessed by qPCR. ▲*P<0.05*, ▲▲*P<0.01*

493   *vs.* control group.

494   **Figure 5** Sulforaphene prevented the effects of METTL3 overexpression on COV362 cells. (A)

495   Cell proliferation of COV362 cells was measured using CCK-8 assay at 24h, 48h, 72h, and 96h.

496   (B) Cell proliferation was also assessed by clone formation assays in METTL3-overexpressed

497   COV362 cells treated with high-dose sulforaphene. (C) Flow cytometry results show that the

498   effects of sulforaphene increased cell apoptosis in the COV362 cells with METTL3

499   overexpression. (D) The expression level of FAS, FADD, p-FADD, Bcl-2, Bax, and Cleaved

500   Caspase-3 in Sul-treated COV362 cells with METTL3 overexpression was determined by

501   western blot. ▲*P<0.05*, ▲▲*P<0.01 vs.* pcDNA3.1 group; *P<0.05, **P<0.01 vs.* pcDNA3.1-

502   METTL3 group.

Figure 1

Figure 1

Figure 1 Identification of methylation-associated genes in endometrioid ovarian cancer. (A) Representative heatmap of differentially expressed genes between the endometrioid ovarian cancer (EOC) and ovarian endometriosis (OE). (B) Gene Ontology (GO) analysis of differentially expressed genes. (C) Kyoto Encyclopedia of Genes and Genomes (KEGG) analysis of differentially expressed genes. (D) Representative heatmap of methylation-associated genes. (E) Relative expression of methylation-associated genes METTL3, ELF3, IGF2BP2, FTO, and METTL14 in EOC and OE tissues. $^{*}P<0.05$, $^{**}P<0.01$ vs. OE group.

Figure 2

Figure 2

Figure 2 Effect of METTL3 on COV362 cell proliferation. (A, B) Relative expression of METTL3 in COV362 cells transfected with siRNA against METTL3 or pcDNA3.1 overexpressed METTL3 was assessed by qPCR and Western blot analysis, respectively. (C) The viability of cells was evaluated by a CCK-8 assay. (D) Colony formation assays were performed in COV362 cells treated with si-NC, si-METTL3, pcDNA3.1, or pcDNA3.1-METTL3. (E) Representative images of the cell cycle in COV362 cells after silencing METTL3 or elevating METTL3 were analyzed by flow cytometry. ▲*P<0.05*, ▲▲*P<0.01 vs.* si-NC group; *P<0.05*, **P<0.01 vs.* PcDNA3.1 group.

A

B

C

D

E
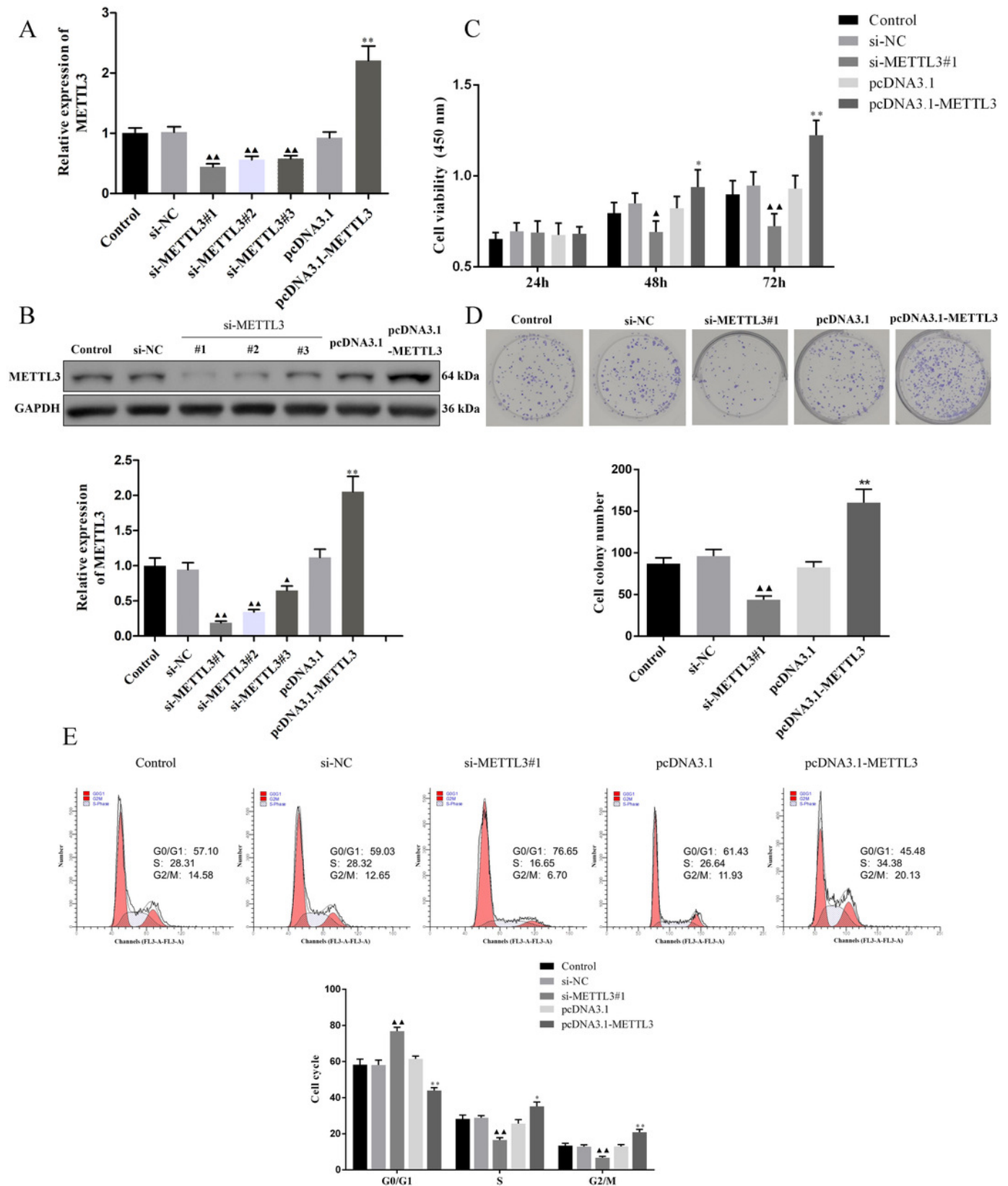
Figure 3

Figure 3

Figure 3 Effect of METTL3 on COV362 cell apoptosis. (A) Representative images of cell apoptosis in COV362 cells after silencing METTL3 or elevating METTL3 were analyzed by Tunel staining. scale bar=50 μm. (B) FAS, FADD, p-FADD, Caspase-8, Caspase-3, Bcl-2, and Bax protein expressions were determined in COV362 cells with METTL3 knock-down or overexpression through western blotting. ▲*P<0.05*, ▲▲*P<0.01 vs.* si-NC group; **P<0.05*, ***P<0.01 vs.* PcDNA3.1 group.

A

B
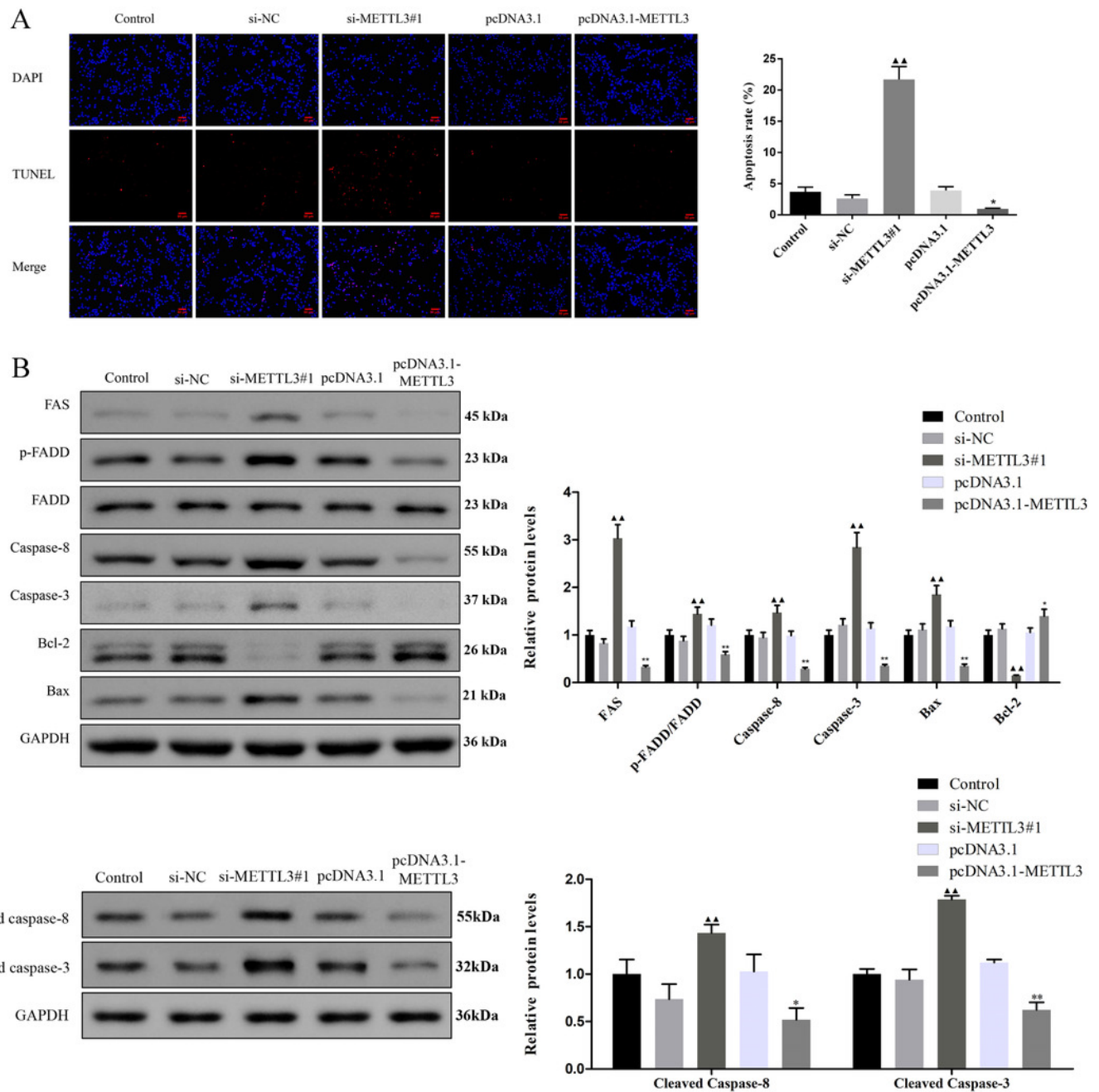
Figure 4

Figure 4

Figure 4 Sulforaphene promoted cell apoptosis of COV362 cells. (A) CCK-8 analysis suggested that the cell viability of COV362 cells was inhibited by a dose-dependent manner of sulforaphene (Sul) treatment. (B) Representative pictures of apoptosis of Sul-treated COV362 cells that were measured by FACS analysis. (C) The relative apoptosis rate of COV362 cells treated with the different concentrations of Sul. (D) Effect of different concentrations of Sul on IGF2BP2, FAS, KRT8, and METTL3 mRNA levels, as assessed by qPCR. ▲*P<0.05*, ▲▲*P<0.01 vs.* control group.

A

24h   36h   48h

IC50=67.96μM   IC50=65.59μM   IC50=57.93μM

B

Control   Sul (20 μM)

Sul (40 μM)   Sul (60 μM)

C

D
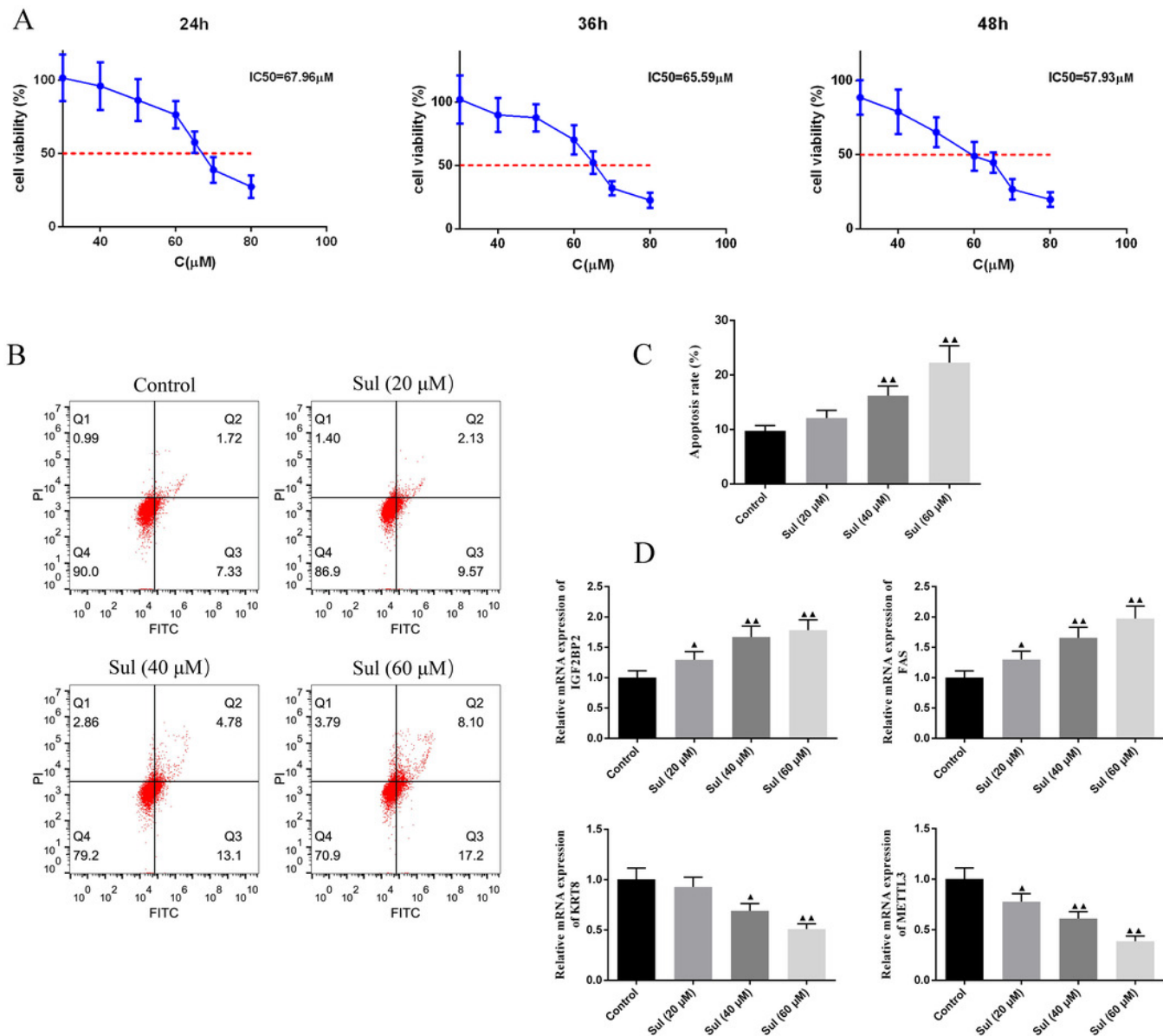
Figure 5

Figure 5

Figure 5 Sulforaphene prevented the effects of METTL3 overexpression on COV362 cells. (A) Cell proliferation of COV362 cells was measured using CCK-8 assay at 24h, 48h, 72h, and 96h. (B) Cell proliferation was also assessed by clone formation assays in METTL3-overexpressed COV362 cells treated with high-dose sulforaphene. (C) Flow cytometry results show that the effects of sulforaphene increased cell apoptosis in the COV362 cells with METTL3 overexpression. $^{\blacktriangle}P<0.05$, $^{\blacktriangle\blacktriangle}P<0.01$ vs. pcDNA3.1 group; $^{*}P<0.05$, $^{**}P<0.01$ vs. pcDNA3.1-METTL3 group.

A

pcDNA3.1
pcDNA3.1-METTL3
pcDNA3.1-METTL3+Sul (60 μM)

C

pcDNA3.1   pcDNA3.1-METTL3   pcDNA3.1-METTL3+ +Sul (60 μM)

B

pcDNA3.1   pcDNA3.1-METTL3   pcDNA3.1-METTL3+ +Sul (60 μM)

D

pcDNA3.1
pcDNA3.1-METTL3
pcDNA3.1-METTL3+ Sul (60 μM)

pcDNA3.1   pcDNA3.1-METTL3   pcDNA3.1-METTL3+ Sul (60 μM)

FAS	38kDa
FADD	28kDa
p-FADD	23kDa
Bcl-2	26kDa
Bax	21kDa
Cleaved caspase-3	32kDa
GAPDH	36kDa